Cytosolic interaction of type III human CD38 with CIB1 modulates cellular cyclic ADP-ribose levels

Jun Liu[a,1], Yong Juan Zhao[a,1,2], Wan Hua Li[a], Yun Nan Hou[a], Ting Li[a], Zhi Ying Zhao[a], Cheng Fang[a], Song Lu Li[a], and Hon Cheung Lee[a,2]

[a]Laboratory of Cytophysiology, Key Laboratory of Chemical Genomics, Peking University Shenzhen Graduate School, Shenzhen 518055, China

Edited by Peter Cresswell, Yale University School of Medicine, New Haven, CT, and approved June 23, 2017 (received for review March 6, 2017)

CD38 catalyzes the synthesis of the Ca^{2+} messenger, cyclic ADP-ribose (cADPR). It is generally considered to be a type II protein with the catalytic domain facing outside. How it can catalyze the synthesis of intracellular cADPR that targets the endoplasmic Ca^{2+} stores has not been resolved. We have proposed that CD38 can also exist in an opposite type III orientation with its catalytic domain facing the cytosol. Here, we developed a method using specific nanobodies to immunotarget two different epitopes simultaneously on the catalytic domain of the type III CD38 and firmly established that it is naturally occurring in human multiple myeloma cells. Because type III CD38 is topologically amenable to cytosolic regulation, we used yeast-two-hybrid screening to identify cytosolic Ca^{2+} and integrin-binding protein 1 (CIB1), as its interacting partner. The results from immunoprecipitation, ELISA, and bimolecular fluorescence complementation confirmed that CIB1 binds specifically to the catalytic domain of CD38, in vivo and in vitro. Mutational studies established that the N terminus of CIB1 is the interacting domain. Using shRNA to knock down and Cas9/guide RNA to knock out CIB1, a direct correlation between the cellular cADPR and CIB1 levels was demonstrated. The results indicate that the type III CD38 is functionally active in producing cellular cADPR and that the activity is specifically modulated through interaction with cytosolic CIB1.

CD38 | cyclic ADP-ribose | membrane topology | calcium signaling | CIB1

Cyclic ADP-ribose (cADPR) is a second-messenger molecule regulating the endoplasmic Ca^{2+} stores in a wide range of cells spanning three biological kingdoms (1–4). Equally widespread is the enzyme activity that cyclizes nicotinamide-adenine dinucleotide (NAD) to produce cADPR (5). The first fully characterized enzyme was the ADP-ribosyl cyclase, a small soluble protein in *Aplysia* (6). It was thus surprising that the soluble cyclase shows sequence homology with the carboxyl (C-) domain of a mammalian membrane protein, CD38, a surface antigen first identified in lymphocytes (7). Subsequent work shows that CD38 is indeed a novel enzyme catalyzing not only the synthesis of cADPR but its hydrolysis to ADP-ribose as well (8, 9). Gene ablation studies establish that CD38 is the dominant enzyme in mammalian tissues responsible for metabolizing cADPR and is important in regulating diverse physiological functions, ranging from neutrophil chemotaxis to oxytocin release and insulin secretion (10–12).

It is generally believed that CD38 is a type II protein with a single transmembrane segment and a short amino(N)-tail of 21 residues extending into the cytosol, whereas the major portion of the molecule, its catalytic C-domain, is facing outside (13). This membrane topology seems paradoxical to CD38 functioning as a signaling enzyme producing an intracellular messenger. A vesicular mechanism has been proposed, positing that CD38 can be endocytosed, together with transport proteins, into endolysosomes. The transporters can then mediate the influx of substrates for CD38 and efflux of cADPR from the endolysosomes to act on the endoplasmic Ca^{2+} stores (14, 15).

Recently, we have shown that CD38, in fact, can exist in two opposite membrane orientations, not only in the expected type II orientation but also in the opposite type III orientation, with the catalytic C-domain facing the cytosol (16). We further establish that the most critical determinants of the topology are the positive charges in the tail next to the transmembrane segment (17). The type III CD38 is fully active in raising the cADPR levels in cells. In this study, we developed a dual-epitope protein identification (DepID) method with high specificity and sensitivity for type III CD38. With it, we confirmed and quantified the intracellular type III CD38 in human multiple myeloma cells. Its regulation was explored using yeast-two-hybrid screening. A cytosolic protein, Ca^{2+} and integrin-binding protein 1 (CIB1), was identified and shown to interact specifically with the catalytic C-domain of the type III CD38. We further showed that the type III CD38 is functionally active in producing cellular cADPR, the levels of which directly correlate with the CIB1 levels. The results substantiate the type III signaling mechanism of CD38 (1, 18).

Results

Development of a DepID Assay for Type III CD38. We have advanced the notion that CD38 exists naturally in both type II and type III orientations, resolving the topological issue surrounding its enzymatic synthesis of the intracellular messenger molecule cADPR. We have shown that mutating the positively charged residues in the N-terminal tail segment of the molecule to negative changes the membrane orientation of CD38 from type II, expressing on the cell surface, to type III, which is localized mostly in the endoplasmic reticulum (ER) (16, 17). An important point that remains to be established is that the intracellular type III CD38 is naturally present in cells.

Significance

This study addresses a topological paradox in Ca^{2+} signaling mediated by cyclic ADP-ribose (cADPR). The messenger is synthesized by CD38, thought to be a type II ectoenzyme. Instead, we show that it exists naturally in two opposite membrane orientations and that the type III, with its catalytic domain facing the cytosol, is active in producing cellular cADPR. Its topology was resolved by a technique simultaneously targeting dual epitopes for protein identification, which identifies the intracellular type III CD38 unambiguously. It is also shown that its cADPR-synthesizing activity is regulated by cytosolic interactions with Ca^{2+} and integrin-binding protein 1 (CIB1). The results indicate that membrane proteins are not necessarily expressed with only one unique membrane orientation set by sequence motifs as generally believed.

Author contributions: Y.J.Z. and H.C.L. designed research; J.L., Y.J.Z., W.H.L., Y.N.H., T.L., Z.Y.Z., C.F., and S.L.L. performed research; J.L., Y.J.Z., and H.C.L. analyzed data; and J.L., Y.J.Z., and H.C.L. wrote the paper.

The authors declare no conflict of interest.

This article is a PNAS Direct Submission.

[1]J.L. and Y.J.Z. contributed equally to this work.

[2]To whom correspondence may be addressed. Email: zhaoyj@pkusz.edu.cn or leehoncheung@gmail.com.

This article contains supporting information online at www.pnas.org/lookup/suppl/doi:10.1073/pnas.1703718114/-/DCSupplemental.

It is anticipated that the abundance of type III CD38 in cells would be much lower than the abundance of dominant type II, obligating the development of a new method for detection with high sensitivity and specificity. Additionally, the method must be able to distinguish its membrane topology definitively. The design of such a method is diagrammed in Fig. 1*A*. Type III CD38 in the ER should have its catalytic-terminal domain facing the cytosol. We targeted two separate epitopes on the C-domain simultaneously using two different nanobodies (Nb-1053 and Nb-551) that we have previously generated (19) (Fig. S1). Crystallography identifies a 3D array of 22 or 23 different residues comprising each epitope (19), making the combination unique to the protein (CD38) that possesses both. The nanobodies were fused with the N-terminal (LucN) or C-terminal (LucC) fragment of *Gaussia princeps* luciferase, respectively. Simultaneous binding of the two nanobodies to the same C-domain of the CD38 molecule allows the two complementing luciferase fragments to get close enough to reconstitute an active enzyme, producing luminescence in the presence of the substrate coelenterazine (20). This approach of using dual epitopes for protein identification (DepID) ensures high specificity, whereas the luminescence detection provides the high sensitivity required.

The topological determinant of the method resides in the cytosolic expression of the Luc-Nb probes, which dictates that only the type III CD38 with its C-domain facing the cytosol can be detected. The amino acid sequences of the designed probes were analyzed with "topology prediction" tools (www.expasy.org/tools) to ensure that there was no potential organelle-targeting signal in the sequence. The constructs were transfected into HEK293 cells. As shown in Fig. 1*B* and Fig. S2, the cytosolic expression of the probes was verified by immunofluorescence microscopy using antibodies against the tags in the probes (HA or Flag; Fig. 1 *A* and *B*). Further support came from digitonin treatment that permeabilized the plasma membrane, resulting in the release of most of the cytosolic probes to the supernatants (Fig. 1*C*). In contrast, GRP78, an ER lumen protein, was retained in the pellets. As a positive control, cells expressing a soluble form of CD38 (sCD38) likewise released most of the molecule to the supernatant after digitonin permeabilization.

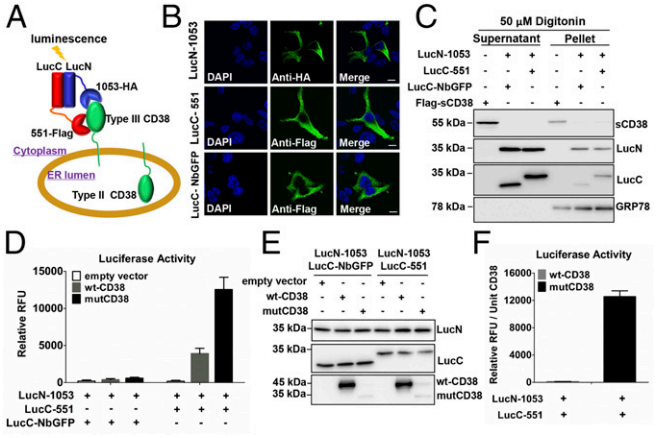

Fig. 1. Detection of type III CD38 in HEK293 cells by the DepID assay. (*A*) Schematic diagram of the DepID assay for type III CD38. Cytosolic probes were constructed by splicing luciferase fragments (LucN or LucC) to nanobodies (1053 or 551) targeting two different epitopes of the C-domain of CD38. Simultaneous binding of both probes to the same type III CD38 reconstitutes the active luciferase and produces luminescence. (*B*) Confocal fluorescence micrographs of HEK293 cells expressing HA-tagged LucN-1053, Flag-tagged LucC-551, or LucC-NbGFP and stained with anti-HA or anti-Flag. (Scale bars: 10 μm.) (*C*) Release of the DepID probes by membrane permeabilization. HEK293 cells stably expressing DepID probes or Flag-sCD38 (a cytosolic control) were permeabilized by 50 μM digitonin, and the supernatant and pellet were analyzed by Western blot, with GRP78 as an ER control. (*D*) DepID assay in HEK293 cells. The cells stably expressing DepID probes were transfected with wt-CD38, mutCD38, or empty vector, separately. Luminescence [relative fluorescent units (RFU)] was measured after addition of 20 μM coelenterazine. (*E*) Expression of DepID probes and CD38 in the cells indicated in *D* was measured by Western blots. (*F*) Luminescence was normalized to the CD38 amounts in the corresponding cells.

The method was then applied to the HEK293 cells expressing type III mutant CD38 (mutCD38; Fig. 1 *D–F*) that was constructed by mutating the positive residues in the N-terminal tail sequence to negative (16). The cells also contained the DepID luciferase probes. As shown in Fig. 1*D*, large luminescence signals were detected, indicating the binding of the two probes to the type III CD38 and reconstituting the active luciferase. As a negative control, one of the probes (LucC-551) was replaced with one containing a nanobody against an irrelevant protein, GFP (LucC-NbGFP; Fig. 1*E*, *Middle*, lanes 1–3), and no luminescence was detected (Fig. 1*D*), even though the amounts of luciferase probes expressed in all of the cells were essentially identical (Fig. 1*E*). The results indicate that the simultaneous binding of two probes to the same type III CD38 molecule is required for generating the luminescence. Likewise, control cells not expressing CD38 (empty vector; Fig. 1*E*) also produced no luminescence (Fig. 1*D*).

Fig. 1*D* also shows that cells overexpressing large amounts of wild-type CD38 (wt-CD38) compared with mutCD38 (Fig. 1*E*) produced only very modest luminescence signals. This result was not due to variation in the amount of probes expressed, because the amounts were essentially identical in all cells (Fig. 1*E*). The results are consistent with the fact that wt-CD38 is known to be mainly expressed on the cell surface as a type II protein (21). When normalized to the amounts of CD38 expressed, it can be seen (Fig. 1*F*) that cells expressing mutCD38 produced more than 100-fold luminescence signal compared with cells expressing wt-CD38. These results verify that the DepID method is highly specific for type III CD38 and has high sensitivity. That cells transfected with a wt-CD38 construct could produce modest luminescence indicates that significant amounts of type III CD38 are normally coexpressed and coexist with type II CD38.

Endogenous Type III CD38 Exists in Multiple Myeloma Cells. With the verification of the DepID method, it was then applied to two multiple myeloma cell lines derived from patients to determine if type III CD38 is naturally expressed in cells. Both LP-1 and OPM2 endogenously express high levels of CD38 (19). Cell lines, based on LP-1 and OPM2, stably expressing LucN-1053 and LucC-551 were generated. Western blots validated the expression of the probe proteins, as well as CD38, the expression level of which was much higher in LP-1 cells than in OPM2 cells (Fig. 2 *A* and *C*). Fig. 2 *B* and *D* show that high luminescence was readily detected in both cell types, whereas no luminescence was detected in the negative controls with LucC-NbGFP. Comparing OPM2 and LP-1 cells, OPM2 produced much higher luminescence even with much less CD38 expressed (compare Fig. S3*D*), indicating that most of it was intracellular type III. To substantiate the DepID method further, the CRISPR-Cas9 technique was used to delete CD38 in the LP-1 cells (22). Genomic sequencing (Fig. S3*A*), Western blot analyses (Fig. 2*A* and Fig. S3*B*, *Inset*), and cell surface staining (Fig. S3*C*) confirmed that the cells expressed no full-length CD38. The luminescence signal was likewise greatly suppressed (Fig. 2*B*). The residual signals might be due to a slight contamination with wild-type cells or some unknown splicing form of CD38 that was active but not deleted by CRISPR targeting (Fig. S3 *A* and *B*). We further measured the cADPR levels in the two cell lines. After normalizing the amounts of CD38 expressed in each cell line, the results showed that OPM2 produced cADPR more efficiently (Fig. 2*E*, left scale, black) than LP-1. The much higher amounts of CD38 in LP-1 cells did result in higher cADPR contents when normalized to total protein (Fig. 2*E*, right scale,

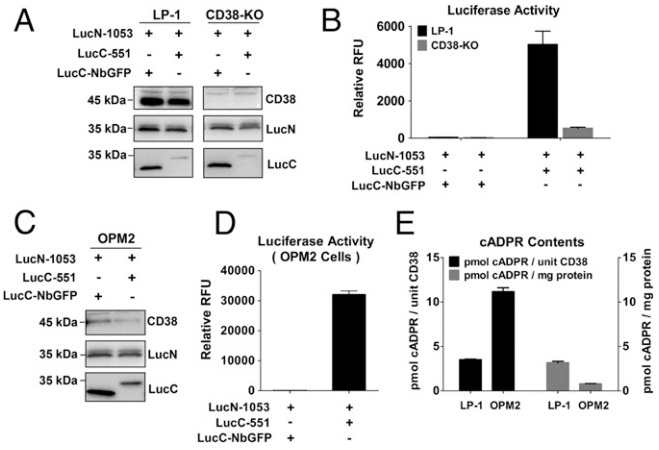

Fig. 2. Endogenous type III CD38 in multiple myeloma cells detected with the DepID assay. (*A*) Western blots of wild-type and CD38-KO LP-1 cells stably expressing DepID probes. (*B*) Luminescence measurement in the LP-1 and CD38-KO cells as described in *A*. (*C*) Western blots of OPM2 cells stably expressing DepID probes. (*D*) Luminescence measurement in the OPM2 cells as described in *C*. (*E*) Intracellular cADPR in the cell lines. Amounts of cADPR were normalized either to the amounts of CD38 expressed (*Left*) or to total protein (*Right*). Data are representative of three independent experiments.

gray). This result indicates that although both type II CD38 and type III CD38 contribute in producing the intracellular cADPR, the type III form is more efficient, consistent with our previous results (16, 17).

Identification of CIB1 as a Specific Interacting Partner of CD38. The natural existence of intracellular type III CD38 with its C-domain facing the cytosol should allow ready modulation of its catalytic activity, and thus cellular cADPR levels, by many of the cytosolic regulatory mechanisms. To identify regulatory proteins that bind to and interact with the C-domain of the type III CD38, we used the yeast-two-hybrid approach (*SI Materials and Methods*). The 30-kDa C-domain of CD38 (sCD38) was used as bait to screen a human leukocyte library (Clontech). Ten positive clones were obtained, and all encoded the same full-length CIB1 (23). It is a cytosolic soluble protein of 183 residues having two high-affinity Ca^{2+}-binding sites with the EF-hand motifs (24) (Fig. S4).

The screening was repeated using a different library, a human spleen library (Clontech). For bait, we used an enzymatically inactive mutant of sCD38, by mutating the catalytic residue of sCD38 from glutamate 226 to glutamine [sCD38 (E226Q)] (25, 26). This change was made to avoid possible interference of the enzymatic product, cADPR, during the screening. Nine positive clones were obtained, and five of them were again positively identified as CIB1.

To demonstrate directly the interaction between the two proteins, CIB1 was expressed in *Escherichia coli* and sCD38 was expressed in yeast (26), and both were purified and verified (Fig. 3*A*). CIB1 was attached to an ELISA plate and incubated with increasing amounts of sCD38. After washing, the amounts of sCD38 specifically bound were assayed using anti-CD38 and peroxidase-conjugated anti-rabbit IgG. As shown in Fig. 3*B*, *Left*, saturable binding of sCD38 to CIB1 was observed. A control using BSA instead of CIB1 showed no signal. Similar results were obtained by attaching sCD38 to the surface and probing with increasing amounts of CIB1. Again, saturable binding was observed (Fig. 3*B*, *Right*).

Intracellular Interaction of CD38 with CIB1. To show that the two proteins can interact inside cells, we used a line of HEK293T cells stably expressing Flag-tagged sCD38 in the cytosol (Flag-sCD38) (16, 27). After transfection with HA-tagged CIB1 and immunoprecipitation (IP) with anti-Flag, a prominent band was clearly present in cells expressing Flag-sCD38 [Fig. 4*B* and Fig. S5*A*, IP:anti-Flag, anti-HA] but not in control cells (Fig. 4*A*, HEK293T). The precipitates and total cell lysate were also analyzed using anti-CD38 or anti-Flag, which confirmed the presence of CD38 in the Flag-sCD38–expressing cells, but not in the control cells. The amounts of CD38 present in cells transfected with the vector with or without CIB1 were similar, which also served as an internal control for input of IP and gel loading.

Fig. S5*B* shows the results of the complementary experiment. The same Flag-sCD38 cells were transfected with either vector as a control or with CIB1-HA, but IP was done using anti-HA instead. Only cells expressing CIB1-HA showed the presence of CD38 (Fig. S5*B*, IP:anti-HA, anti-CD38) and CIB1 (Fig. S5*B*, IP: anti-HA, anti-CIB1) in the precipitates.

HEK293T cells stably expressing mutCD38 were transfected with CIB1-HA to determine if it could really interact with the transmembrane type III CD38. Cell lysates were immunoprecipitated using anti-Flag or anti-CD38, and the Western blots were probed using anti-HA. Fig. 4*C* and Fig. S5*C* show the clear presence of CIB1 in the precipitates (IP, anti-HA). Anti-Flag or anti-CD38 staining showed similar amounts of CD38 were present in both (Fig. 4*C* and Fig. S5*C*), serving as an internal control for input of IP and gel loading. A complementary experiment using anti-HA (CIB1) for the IP likewise confirmed that CD38 was present in the precipitates (Fig. S5*D*, IP:anti-HA, anti-CD38).

Identification of the N Terminus of CIB1 as Its CD38-Interacting Region. Mutational analysis was then used to identify the interacting domain in CIB1. Mutating Gly2 in CIB1 to alanine eliminated its association with all forms of CD38 (Fig. 4 *B* and *C* and Fig. S6*C*, IP: anti-Flag, anti-HA, lane 3). No or little mutant CIB1 was detected in the immunoprecipitates of cytosolic CD38 (Fig. 4 *B* and *D* and Fig. S6*A*), mutCD38 (Fig. 4 *C* and *D* and Fig. S6*B*) and wt-CD38 (Fig. S6*C*). In contrast, mutating Ser78 to alanine (Fig. 4 *B* and *C* or Fig. S6, IP:anti-Flag or anti-CD38, anti-HA, lane 4), a potential phosphorylation site (28), was innocuous for the interaction. The amounts of the mutant CIB1 in cells expressing cytosolic CD38 (Fig. 4*B*), mutCD38 (Fig. 4*C*), and wt-CD38 (Fig. S6*C*) were similar to amounts expressing wild-type CIB1 (Cell Lysate, Anti-HA). The results indicate CIB1 interacts with the type III CD38 through its N-terminal region, which is on the surface (Fig. S4, blue). The innocuous Ser78 is, on the other hand, located in the interior (Fig. S4, orange). It is of interest to note that Gly2 is known to be the site for myristoylation of CIB1 (29), suggesting that the type III CD38, being a membrane protein, may have a

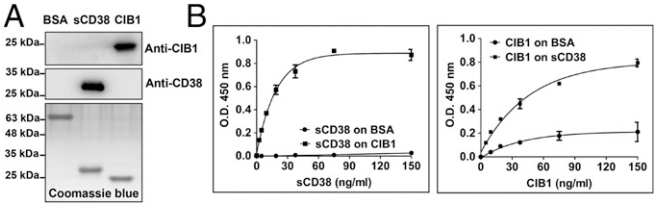

Fig. 3. In vitro interaction between recombinant CIB1 and sCD38. (*A*) Western blots and protein gel of the purified recombinant CIB1 and sCD38 used for ELISA. (*B*) In vitro binding between sCD38 and CIB1 analyzed by ELISA. (*Left*) Microtiter plates were coated with CIB1 or BSA and then incubated with increasing concentrations of sCD38. The amounts of sCD38 retained were measured using polyclonal anti-CD38. (*Right*) Similar to *Left* except that the plate was coated with sCD38 and incubated with increasing CIB1. The mean ± SEM of one representative experiment performed in triplicate is shown. O.D., optical density.

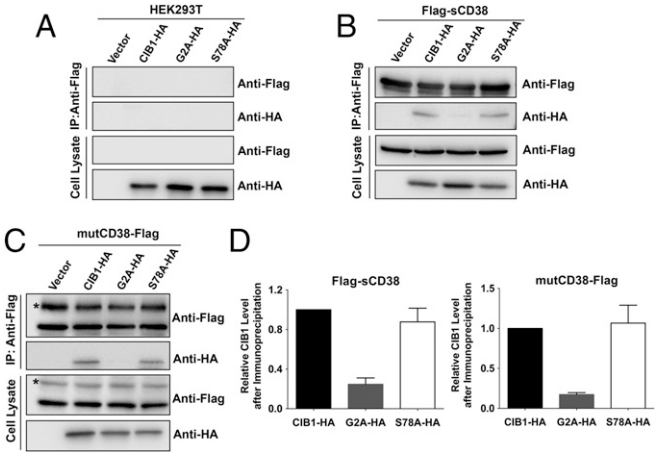

Fig. 4. Mutational study on CIB1 interacting with type III CD38. HEK293T cells (*A*) or the cells stably expressing Flag-tagged sCD38 (*B*) or Flag-tagged mutCD38 (*C*) were transfected with empty vector, HA-tagged CIB1 (CIB1-HA), G2A (G2A-HA), or S78A mutant (S78A-HA). CD38 in the lysates was immunoprecipitated, followed by Western blots with anti-Flag or anti-HA. The label (*) in *C* indicates type II CD38. Results from one representative experiment are shown. (*D*) Quantification of CIB1-HA, G2A-HA, or S78A-HA in the gels after IP shown in *B* and *C*. Values are represented as the mean ± SEM ($n = 4$). Additional results are shown in Fig. S6.

preference for the myristoylated form of CIB1 due to its membrane localization or conformational difference.

Visualization of Intracellular Interaction of CD38 with CIB1 by Bimolecular Fluorescence Complementation. The bimolecular fluorescence complementation (BiFC) technique (30) was then used to visualize CIB1 interacting with the type III CD38. The technique is based on the structural complementation of two nonfluorescent fragments, N-terminal (VN173) and C-terminal (VC155), of a fluorescent protein, Venus, that are fused, respectively, to a pair of interacting proteins. The binding of the two interacting proteins brings the two nonfluorescent fragments together and reconstitutes the fluorescence. Constructs were made by fusing VN173 to the C terminus of mutCD38 and VC155 to the C terminus of CIB1 (*SI Materials and Methods*). HEK293T cells were cotransfected with the two constructs, and, as shown in Fig. 5*A* and Fig. S7*A*, BiFC was observed in localized regions resembling the ER inside the live cells.

Fig. 5*B* and Fig. S7*B* show the positive control using Fos and Jun, which are known to interact inside the cell nucleus (31). Indeed, BiFC was observed only in the nucleus of the cells cotransfected with bJun-VN173 and bFos-VC155 (Fig. 5*B* and Fig. S7*B*, *Upper*). Truncated Fos (bFosΔZIP-VC155) loses its ability to interact with Jun, and no BiFC was observed (negative control; Fig. 5*B* and Fig. S7*B*, *Lower*).

Cellular distribution of CIB1-HA and the type III CD38 was visualized by immunofluorescence staining using anti-HA and anti-CD38. Fig. 5*C* and Fig. S7*C* show that the BiFC signals colocalized with the type III CD38 (mutCD38) in regions consistent with the ER. The distribution of CIB1 confirmed that it is a cytosolic molecule, but the BiFC signal was observed only in regions where it colocalized with the type III CD38.

As mentioned above, we have previously constructed the catalytic C-domain of CD38 as a soluble cytosolic protein (sCD38) (27). If CIB1 indeed binds to the C-domain, the BiFC pattern should be cytosolic in cells expressing sCD38 instead of mutCD38. Such was indeed the case, as shown in Fig. 5*D* and Fig. S7*D*. HEK293T cells were cotransfected with VN173-sCD38 and CIB1-VC155. The BiFC pattern was clearly cytosolic, essentially the same as the distribution of both CIB1 and sCD38. The fact that the BiFC pattern is determined by the subcellular distribution of CD38 strongly substantiates the authenticity of the technique for visualizing the two interacting proteins in cells.

BiFC probes were also constructed for the G2A mutant of CIB1 described above and an additional mutant with the first five residues truncated. Consistently, the percentages of the mutCD38 cells transfected with these constructs and showed BiFC signals greatly decreased (Fig. S8).

The colocalization of mutCD38 and the BiFC signal was quantified by scatter plot. In Fig. 5*E*, the fluorescence intensities of mutCD38 and BiFC at each pixel of the image (Fig. 5*C*) were plotted in a 2D scattered graph using the program ImarisColoc. For perfect colocalization, points should fall on a straight line, the slope of which depends on the ratio of the fluorescence of the two signals. Fig. 5*E* shows that the points generally follow a straight line, indicating good colocalization. Fig. 5*F* shows similarly good colocalization for sCD38 and BiFC.

Colocalization for a population of cells was further analyzed using the Image J (NIH) plugin JACoP (*SI Materials and Methods*). Pearson's correlation coefficient (PC) and Menders' coefficient (M_1 and M_2) were calculated for the mutCD38 and sCD38, as well as their respective BiFC signals. Fig. 5*G* shows the values of PC, M_1, and M_2 are all close to 1 for both mutCD38 vs. BiFC and sCD38 vs. BiFC (Fig. 5*G*), indicating good colocalization.

The above results, using three entirely different techniques, all confirmed that CIB1 specifically interacts with CD38 in vitro, as well as in live cells. The finding that the full-length type III CD38, as well as the catalytic C-domain of CD38, specifically interacts with a cytosolic regulatory protein also provides strong support for the type III signaling mechanism of CD38.

CIB1 Modulates the Intracellular cADPR Level. According to the results from the DepID assay, both LP-1 and OPM2 can be used to study the regulatory mechanism of endogenous type III CD38. We chose LP-1 because it endogenously expresses both CIB1 and CD38 (Fig. 6*A*, Cell Lysate, lane 2), making the results more

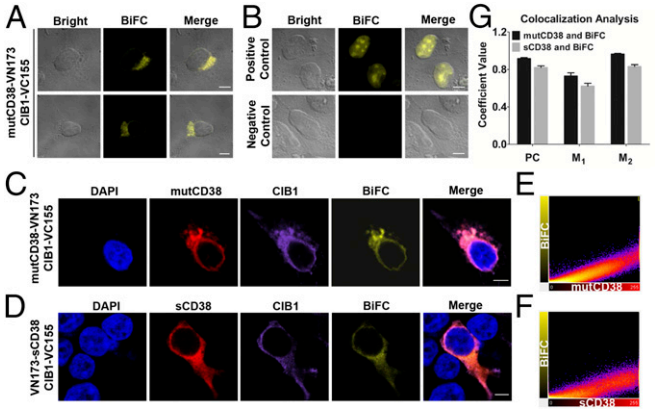

Fig. 5. Visualization of intracellular association between CIB1 and type III CD38 using BiFC. (*A*) BiFC of mutCD38-VN173 and CIB1-VC155. (*B*) BiFC of bJun-VN173 and bFos-VC155 (positive control) or bJun-VN173 and bFosΔZIP-VC155 (negative control). (*C* and *D*) BiFC with the immunostaining signals of CIB1 (anti-HA, purple, Alexa Fluor 647) and mutCD38 (*C*; red, Alexa Fluor 555) or sCD38 (*D*; red, Alexa Fluor 555). BiFC fluorescence is shown in yellow, and nuclear staining (DAPI) is shown in blue. The merged image shows superposition of CD38, CIB1, and DAPI signals. (*E* and *F*) Colocalization analysis with Imaris software. Scatter-plot pixels correspond to the images shown in *C* and *D*. Complete colocalization results in a pixel distribution along a straight line whose slope will depend on the fluorescence ratio between the two channels. (*G*) PC, M_1, and M_2 were analyzed with JACoP. M_1 is defined as the fraction of mutCD38 (black bars) or sCD38 (gray bars) overlapping BiFC signal; M_2 is defined conversely. Values are shown as the mean ± SEM of 63 mutCD38 cells and 52 sCD38 cells. Additional results are shown in Fig. S7. (Scale bars: *A*–*D*, 5 μm.)

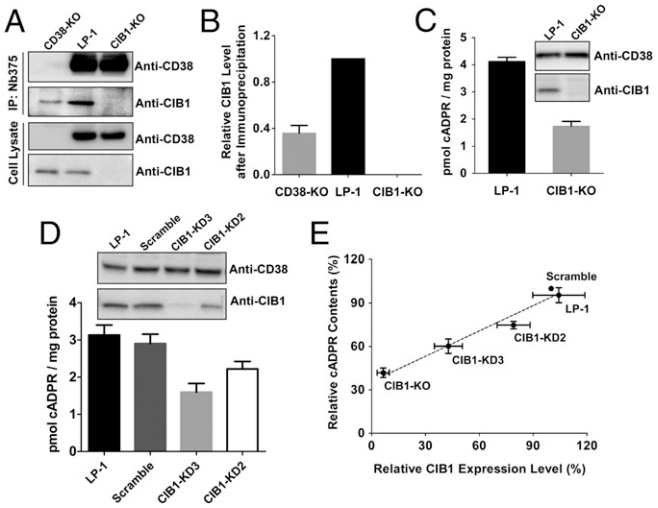

Fig. 6. Correlation between cADPR contents and CIB1 expression levels. (*A*) Co-IP of endogenous CIB1 and CD38 with a nanobody against CD38 (Nb-375). Detection of CIB1 and CD38 was done using anti-CIB1 or anti-CD38, respectively. Additional results are shown in Fig. S9*B*. (*B*) Quantification of CIB1 after IP in similar gels as shown in *A* (mean ± SEM, $n = 5$). The intracellular cADPR contents in wild-type, CIB1-KO (*C*), and CIB1-knockdown (KD) (*D*) LP-1 cells are shown. (*Inset*) Western blots of CD38 and CIB1 in different LP-1 cells. (*E*) Linear correlation ($R^2 = 0.98$) between CIB1 and cADPR contents. Values are presented as the mean ± SEM ($n = 3$).

physiologically relevant. To delete the CIB1 or CD38 gene, guide RNA targeting its exon region was cloned into the CRISPR plasmid lentiCRISPRv2 (32) or pX458 (22), respectively (*SI Materials and Methods*). As described in *Materials and Methods*, cell clones were selected, and sequencing confirmed the deletion (Fig. 3*A* and Fig. S9*A*). Western blot analysis also confirmed that CIB1 or CD38 was not expressed (Fig. 6*A*, Cell Lysate, lane 3, anti-CIB1 and lane 1, anti-CD38).

With these cell lines, we first investigated the interaction between endogenous CD38 and CIB1. As shown in Fig. 6*A* (IP:Nb375), both CD38 and CIB1 could be pulled down in the wild-type LP-1 cells by the immobilized CD38 nanobody, Nb-375, which binds to an epitope overlapping with Nb-1053 (19). Background contamination by endogenous CIB1 during IP was assessed using CD38-KO cells (compare Fig. 2*A*), which showed much less CIB1 signal, and was completely eliminated in the CIB1-KO cells (Fig. 6 *A* and *B*).

The physiological association between CD38 and CIB1 prompted us to explore further the effect on cADPR production, which is one of the main direct functions of CD38 as a signaling enzyme. This analysis was done by depleting CIB1 in LP-1 cells. As shown in Fig. 6*C*, the cADPR contents in the CIB1-KO cells were measured to be greatly reduced to ∼40% of the contents of wild-type LP-1 cells. The CIB1 levels in cells can also be manipulated by using shRNA to reduce the expression of CIB1. Fig. 6*D* shows that the larger the reduction of the CIB1 levels (*Inset*), the larger is the reduction in the cADPR contents.

Combining all of the results in various treated cells with different CIB1 expression levels, there is a direct correlation between the cellular cADPR and CIB1 levels, with a correlation value (R^2) of 0.98 (Fig. 6*E*). Because CIB1 is a cytosolic protein and, as shown above, it binds to the catalytic C-domain of CD38, the results indicate that CIB1 can modulate the enzymatic activity of the endogenous type III CD38 in human myeloma cells. The residual cADPR level in the CIB1-KO cells thus represented the basal cADPR-synthesizing activity of the endogenous type III CD38. Consistently, purified recombinant sCD38 is enzymatically active (8). Interaction with cytosolic CIB1 can thus potentially enhance this basal activity by about two- to threefold.

Discussion

A topological issue has remained unresolved ever since CD38 was established as the dominant enzyme for metabolizing cADPR in mammalian cells and tissues, because the enzymatic activity was presumed to face the extracellular region. An attractive feature of the type III signaling mechanism of CD38 is that it not only renders the issue moot but also provides a new approach for understanding the regulatory mechanism of CD38. The current results showing that the catalytic C-domain of CD38 interacts with a cytosolic regulatory protein, CIB1, and that this interaction leads to modulation of cADPR levels are strongly supportive of the mechanism.

Here, we devised a sophisticated DepID method to establish firmly the natural occurrence of the intracellular type III CD38. The requirement of the presence of dual epitopes greatly increases the specificity of the identification compared with other immunotargeting methods. The use of complementary reconstitution of luciferase ensures not only high sensitivity but also extremely low background. Furthermore, the method detects total type III CD38 present in both the plasma and organellar membranes. In all, DepID is a great improvement and much more definitive than the surface staining assay of the N-terminal tail sequence we previously used (16). The success of DepID in identifying CD38 is a proof of principle for the approach, which can be easily extended for identifying any cellular protein by using appropriate antibodies in the constructs. DepID is also topologically versatile. Here, we directed the expression of the luciferase probes to the cytosol to ensure targeting only the type III CD38 facing the cytosol. With an appropriate targeting sequence inserted into the probes, DepID can be designed to identify luminal proteins in organelles as well. DepID can be a general method of choice for protein identification.

CIB1 is a multifunctional regulatory protein having two high-affinity binding sites for Ca^{2+} with the EF-hand motifs. It has been shown to be involved in regulating Ca^{2+} signaling through binding to the inositol trisphosphate (IP_3) receptor and modulating its ion channel activity (23). Here, we showed that CIB1 interacts with type III CD38 through its N terminus. Mutating Gly2 abolished the interaction, indicating specificity (Fig. 4). Gly2 is also known to be the myristoylation site of CIB1. Considering that CIB1 is a Ca^{2+}/myristoyl switch, changes in intracellular Ca^{2+} may alter its interaction with CD38, resulting in consequential modulation of its enzymatic activity. The mechanistic details are now being explored. It seems unlikely, however, that direct binding of CIB1 to CD38 can alter its catalytic activity via conformational change, because the crystal structure of CD38 shows that it is a rather rigid molecule with six disulfide bridges (26, 33). However, if the binding is at the mouth of the active site pocket, it could lead to changes in the entry and exit of NAD and/or cADPR.

For type III CD38, its catalytic C-domain is in the reducing environment of the cytosol. Some of its disulfide bridges could be disturbed. A possible function of CIB1 could thus be serving as a protein chaperone, preserving the disulfides of CD38 and its enzymatic activity. We have shown that all of the disulfides, except the last one (C287–C296), are important for the cADPR-synthesizing activity of CD38 (27). Mutation of the individual cysteine residues of these disulfides can lead to a 70–80% reduction in activity. By preserving the disulfides, CIB1 can thus effect about a two- to threefold enhancement of the type III CD38 activity, consistent with the extent of enhancement that was observed in this study (Fig. 6).

Another possibility for modulation of the CD38 activity could be through modification of the catalytic domain of CD38. CIB1 is known to interact with a variety of kinases, including ASK1 (34). This fact is relevant because we and others have reported that cADPR synthesis in sea urchin eggs is activated by a cGMP-dependent phosphorylation process (35, 36). A similar mechanism

CELL BIOLOGY

also operates in rat hippocampus (37). In human granulocytes, agonist-induced activation and phosphorylation of CD38 are found to be cAMP-dependent (38). CIB1 can function as an adaptor protein, binding and recruiting various kinases to the proximity of the catalytic domain of CD38 and effecting regulation through phosphorylation. The converse could also be true, because CIB1 is also known to bind calcineurin B, a regulatory subunit of the phosphatase calcineurin (39). Although the exact mechanism of how CIB1 modulates CD38 activity remains to be elucidated, the facts that the type III CD38 naturally exists and a cytosolic regulator, CIB1, is involved in regulating its activity point to a new paradigm for understanding the cADPR/CD38 signaling pathway.

Materials and Methods

Details of the materials and methods used, including the yeast-two-hybrid screen, vector constructions, DepID, immunostaining, and other assays, are available in *SI Materials and Methods*. All relevant data are available from the authors upon request.

ACKNOWLEDGMENTS. We thank Richard Graeff for reading and editing our manuscript. This study was supported by grants from National Science Foundation of China (Grant 31501134 to J.L., Grant 31571438 to Y.J.Z., and Grants 31470815 and 31671463 to H.C.L.) and grants from Shenzhen and Guangdong Governments (Grants JCYJ20150331100801849, JCYJ20160428153800920, JCYJ20160608091848749, ZDSYS201504301539161, KQTD2015071714043444, and 2014B030301003).

1. Lee HC (2012) Cyclic ADP-ribose and nicotinic acid adenine dinucleotide phosphate (NAADP) as messengers for calcium mobilization. *J Biol Chem* 287:31633–31640.
2. Lee HC (2012) The cyclic ADP-ribose/NAADP/CD38-signaling pathway: Past and present. *Messenger (Los Angel)* 1:16–33.
3. Lee HC, Aarhus R, Levitt D (1994) The crystal structure of cyclic ADP-ribose. *Nat Struct Biol* 1:143–144.
4. Lee HC, Walseth TF, Bratt GT, Hayes RN, Clapper DL (1989) Structural determination of a cyclic metabolite of NAD+ with intracellular Ca2+-mobilizing activity. *J Biol Chem* 264:1608–1615.
5. Rusinko N, Lee HC (1989) Widespread occurrence in animal tissues of an enzyme catalyzing the conversion of NAD+ into a cyclic metabolite with intracellular Ca2+-mobilizing activity. *J Biol Chem* 264:11725–11731.
6. Lee HC, Aarhus R (1991) ADP-ribosyl cyclase: An enzyme that cyclizes NAD+ into a calcium-mobilizing metabolite. *Cell Regul* 2:203–209.
7. States DJ, Walseth TF, Lee HC (1992) Similarities in amino acid sequences of *Aplysia* ADP-ribosyl cyclase and human lymphocyte antigen CD38. *Trends Biochem Sci* 17:495.
8. Howard M, et al. (1993) Formation and hydrolysis of cyclic ADP-ribose catalyzed by lymphocyte antigen CD38. *Science* 262:1056–1059.
9. Takasawa S, et al. (1993) Synthesis and hydrolysis of cyclic ADP-ribose by human leukocyte antigen CD38 and inhibition of the hydrolysis by ATP. *J Biol Chem* 268: 26052–26054.
10. Kato I, et al. (1999) CD38 disruption impairs glucose-induced increases in cyclic ADP-ribose, [Ca2+]i, and insulin secretion. *J Biol Chem* 274:1869–1872.
11. Jin D, et al. (2007) CD38 is critical for social behaviour by regulating oxytocin secretion. *Nature* 446:41–45.
12. Partida-Sánchez S, et al. (2001) Cyclic ADP-ribose production by CD38 regulates intracellular calcium release, extracellular calcium influx and chemotaxis in neutrophils and is required for bacterial clearance in vivo. *Nat Med* 7:1209–1216.
13. Jackson DG, Bell JI (1990) Isolation of a cDNA encoding the human CD38 (T10) molecule, a cell surface glycoprotein with an unusual discontinuous pattern of expression during lymphocyte differentiation. *J Immunol* 144:2811–2815.
14. Bruzzone S, et al. (2012) Subcellular and intercellular traffic of NAD+, NAD+ precursors and NAD+-derived signal metabolites and second messengers: Old and new topological paradoxes. *Messenger (Los Angel)* 1:34–52.
15. De Flora A, Zocchi E, Guida L, Franco L, Bruzzone S (2004) Autocrine and paracrine calcium signaling by the CD38/NAD+/cyclic ADP-ribose system. *Ann N Y Acad Sci* 1028: 176–191.
16. Zhao YJ, Lam CM, Lee HC (2012) The membrane-bound enzyme CD38 exists in two opposing orientations. *Sci Signal* 5:ra67.
17. Zhao YJ, Zhu WJ, Wang XW, Zhang LH, Lee HC (2015) Determinants of the membrane orientation of a calcium signaling enzyme CD38. *Biochim Biophys Acta* 1853: 2095–2103.
18. Lee HC, Zhao YJ (2014) The type III calcium signaling mechanism of CD38. *Messenger (Los Angel)* 3:59–64.
19. Li T, et al. (2016) Immuno-targeting the multifunctional CD38 using nanobody. *Sci Rep* 6:27055.
20. Cassonnet P, et al. (2011) Benchmarking a luciferase complementation assay for detecting protein complexes. *Nat Methods* 8:990–992.
21. Mehta K, Shahid U, Malavasi F (1996) Human CD38, a cell-surface protein with multiple functions. *FASEB J* 10:1408–1417.
22. Ran FA, et al. (2013) Genome engineering using the CRISPR-Cas9 system. *Nat Protoc* 8: 2281–2308.
23. White C, Yang J, Monteiro MJ, Foskett JK (2006) CIB1, a ubiquitously expressed Ca2+-binding protein ligand of the InsP3 receptor Ca2+ release channel. *J Biol Chem* 281: 20825–20833.
24. Gentry HR, et al. (2005) Structural and biochemical characterization of CIB1 delineates a new family of EF-hand-containing proteins. *J Biol Chem* 280:8407–8415.
25. Liu Q, et al. (2006) Structural basis for the mechanistic understanding of human CD38-controlled multiple catalysis. *J Biol Chem* 281:32861–32869.
26. Munshi C, et al. (2000) Identification of the enzymatic active site of CD38 by site-directed mutagenesis. *J Biol Chem* 275:21566–21571.
27. Zhao YJ, Zhang HM, Lam CM, Hao Q, Lee HC (2011) Cytosolic CD38 protein forms intact disulfides and is active in elevating intracellular cyclic ADP-ribose. *J Biol Chem* 286:22170–22177.
28. Armacki M, et al. (2014) A novel splice variant of calcium and integrin-binding protein 1 mediates protein kinase D2-stimulated tumour growth by regulating angiogenesis. *Oncogene* 33:1167–1180.
29. Jarman KE, Moretti PA, Zebol JR, Pitson SM (2010) Translocation of sphingosine kinase 1 to the plasma membrane is mediated by calcium- and integrin-binding protein 1. *J Biol Chem* 285:483–492.
30. Shyu YJ, Liu H, Deng X, Hu CD (2006) Identification of new fluorescent protein fragments for bimolecular fluorescence complementation analysis under physiological conditions. *Biotechniques* 40:61–66.
31. Hu CD, Chinenov Y, Kerppola TK (2002) Visualization of interactions among bZIP and Rel family proteins in living cells using bimolecular fluorescence complementation. *Mol Cell* 9:789–798.
32. Sanjana NE, Shalem O, Zhang F (2014) Improved vectors and genome-wide libraries for CRISPR screening. *Nat Methods* 11:783–784.
33. Liu Q, et al. (2005) Crystal structure of human CD38 extracellular domain. *Structure* 13:1331–1339.
34. Yoon KW, et al. (2009) CIB1 functions as a Ca(2+)-sensitive modulator of stress-induced signaling by targeting ASK1. *Proc Natl Acad Sci USA* 106:17389–17394, and erratum (2006) 106:19629.
35. Galione A, et al. (1993) cGMP mobilizes intracellular Ca2+ in sea urchin eggs by stimulating cyclic ADP-ribose synthesis. *Nature* 365:456–459.
36. Willmott N, et al. (1996) Nitric oxide-induced mobilization of intracellular calcium via the cyclic ADP-ribose signaling pathway. *J Biol Chem* 271:3699–3705.
37. Reyes-Harde M, Potter BV, Galione A, Stanton PK (1999) Induction of hippocampal LTD requires nitric-oxide-stimulated PKG activity and Ca2+ release from cyclic ADP-ribose-sensitive stores. *J Neurophysiol* 82:1569–1576.
38. Bruzzone S, et al. (2007) Abscisic acid is an endogenous cytokine in human granulocytes with cyclic ADP-ribose as second messenger. *Proc Natl Acad Sci USA* 104: 5759–5764.
39. Heineke J, et al. (2010) CIB1 is a regulator of pathological cardiac hypertrophy. *Nat Med* 16:872–879.
40. Haataja L, Kaartinen V, Groffen J, Heisterkamp N (2002) The small GTPase Rac3 interacts with the integrin-binding protein CIB and promotes integrin alpha(IIb)beta(3)-mediated adhesion and spreading. *J Biol Chem* 277:8321–8328.
41. Yamniuk AP, Nguyen LT, Hoang TT, Vogel HJ (2004) Metal ion binding properties and conformational states of calcium- and integrin-binding protein. *Biochemistry* 43: 2558–2568.
42. Kubala MH, Kovtun O, Alexandrov K, Collins BM (2010) Structural and thermodynamic analysis of the GFP:GFP-nanobody complex. *Protein Sci* 19:2389–2401.
43. Moffat J, et al. (2006) A lentiviral RNAi library for human and mouse genes applied to an arrayed viral high-content screen. *Cell* 124:1283–1298.
44. Sarbassov DD, Guertin DA, Ali SM, Sabatini DM (2005) Phosphorylation and regulation of Akt/PKB by the rictor-mTOR complex. *Science* 307:1098–1101.
45. Bonifacino JS, Dell'Angelica EC (2001) Immunoprecipitation. *Curr Protoc Cell Biol* Chapter 7:Unit 7.2.
46. Dunn KW, Kamocka MM, McDonald JH (2011) A practical guide to evaluating colocalization in biological microscopy. *Am J Physiol Cell Physiol* 300:C723–C742.
47. Graeff R, Lee HC (2002) A novel cycling assay for cellular cADP-ribose with nanomolar sensitivity. *Biochem J* 361:379–384.